Transportation Research Part C 53 (2015) 93–111

Contents lists available at ScienceDirect

Transportation Research Part C

journal homepage: www.elsevier.com/locate/trc

A multi-path progression model for synchronization of arterial traffic signals

Xianfeng Yang *, Yao Cheng, Gang-Len Chang

Department of Civil & Environmental Engineering, University of Maryland, College Park, USA

ARTICLE INFO

Article history:
Received 20 May 2014
Received in revised form 15 February 2015
Accepted 16 February 2015
Available online 4 March 2015

Keywords:
Critical path
Multi-path progression
Green band
Phase sequence

ABSTRACT

To contend with congestion and spillback on commuting arterials, serving as connectors between freeway and surface-street flows, this paper presents three multi-path progression models to offer progression bands for multiple critical path-flows contributing to the high volume in each arterial link. The first proposed model is a direct extension of MAXBAND under a predetermined phasing plan, but using the path-flow data to yield the progression bands. The second model further takes the phase sequence at each intersection as a decision variable, and concurrently optimizes the signal plans with offsets for the entire arterial. Due to the competing nature of multi-path progression flows over the same green duration, the third model is proposed with a function to automatically select the optimal number of paths in their bandwidths maximization process. The results of extensive simulation studies have shown that the proposed models outperform conventional design methods, such as MAXBAND or TRANSYT, especially for those arterials with multiple heavy path-flows. The research results from this study have also reflected the need to collect more traffic pattern data such as major path-flow volumes, in addition to the typical intersection volume counts.

1. Introduction

Providing two-way signal progression for congested arterials has long been viewed by traffic professionals as one of the most effective control strategies. Over the past several decades, researchers in the traffic control community have proposed a variety of signal progression models (Morgan and Little, 1964; Little, 1966) to maximize the progression bands for the target movements. Depending on the selected measures of effectiveness (MOEs), most of those existing studies have made impressive contributions on mitigating arterial traffic congestion. The effectiveness of all progression-based models, in general, are conditioned on the common traffic pattern where through traffic constitutes the primary volume on the arterial, and consequently turning flows are not the main concern of the signal design. However, for many arterials serving as the connectors between freeway commuting flows and urban traffic networks, the traffic volumes, that need to take these paths comprising both turning and through movements, are likely to be at the same level or even higher than the through volume along the arterial. Thus, depending on the required turning volume at each arterial intersection, the conventional progression design for through traffic flows may not be adequate to contend with the potential queue spillback and resulting stop-and-going conditions, especially for arterials having a short link and bay length between intersections.

* Corresponding author at: 3111 Kim Building, University of Maryland, College Park, MD 20740, USA. Tel.: +1 301 405 2638.
E-mail addresses: xyang125@umd.edu (X. Yang), ycheng09@umd.edu (Y. Cheng), gang@umd.edu (G.-L. Chang).

http://dx.doi.org/10.1016/j.trc.2015.02.010
0968-090X/

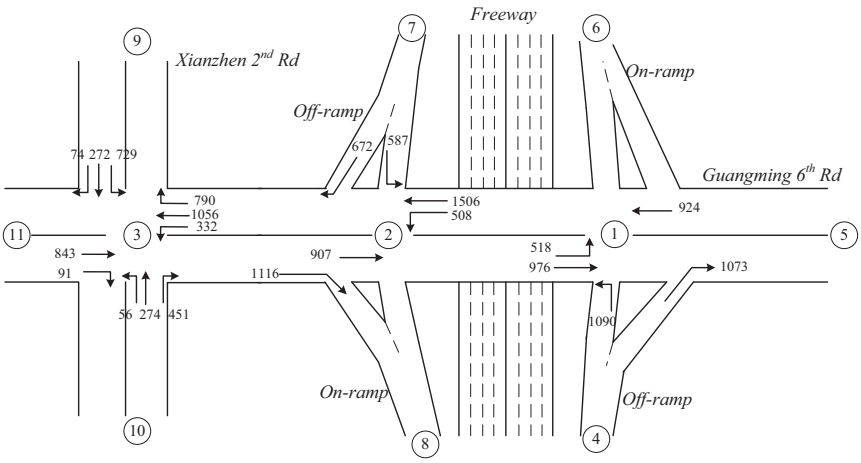

Fig. 1a. An arterial segment and volume distribution in Chupei, Taiwan.

Fig. 1a presents an example of such traffic systems in Chupei, Taiwan, where the arterial segment comprising three intersections to connect a congested commuting freeway and urban network. The heavy turning volumes from-or-to the on-ramp and off-ramps are in conflict with through traffic, and the design of conventional two-way progression often yields both overflow at turning bays and consequently a gridlock for the entire network. A further field survey and analysis has revealed that the traffic patterns along the arterial segment are the collective manifestation of five congested path-flows. As shown in Fig. 1b, Path-1 flows from Node 4 to Node 11 exhibit the highest volume (702 vph), and all vehicles along this path need to first manipulate a turning movement and then join the through traffic on the main arterial. Other primary path-flows, including Path-2 (Node 5 to Node 8), Path-3 (Node 4 to Node 9), and Path-4 (Node 7 to Node 5) also share the common features of having heavy turning volume to merge to the through traffic flows. Moreover, traffic flows on those outbound paths (Paths 1, 2, 3) are in conflict with those inbound paths (Paths 4, 5), inevitably causing the conventional design of two-way progression ineffective. Hence, how to smooth traffic movements on such a congested arterial that serves as a connector between a commuting freeway and primary trip-destination locations is an imperative issue in design of effective urban traffic control.

In review of the literature on arterial traffic control, one may classify most existing studies into two distinct categories: maximizing traffic progression and minimizing total vehicle delay. The core logic of most studies in the former category is to synchronize signals of a common cycle length with optimized offsets on an arterial to facilitate the movement of vehicles over consecutive intersections. Morgan and Little (1964) are the pioneers who first presented a model to maximize the total two-way progression bandwidth on an arterial. Following the same principle, Little (1966) further proposed an advanced model to concurrently optimize the common cycle length, progression speeds, and offsets with integer programming. An

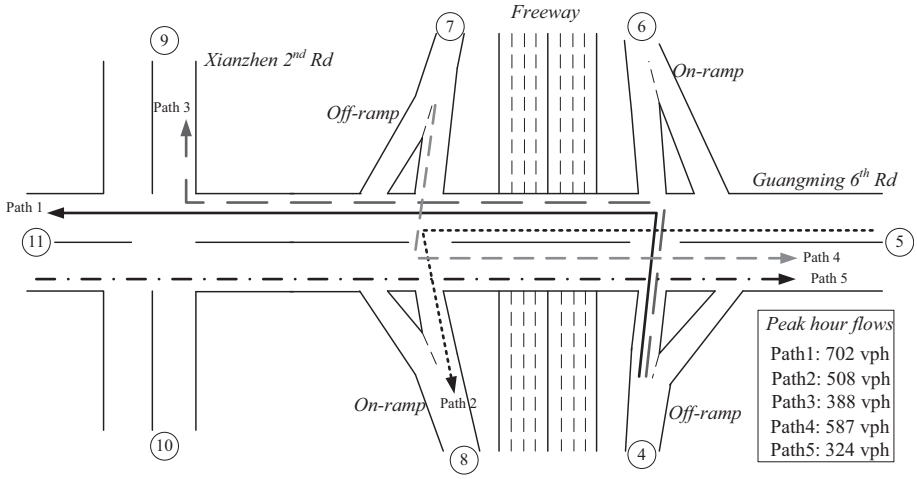

Fig. 1b. Critical traffic paths passing more than two intersections in Chupei, Taiwan.

enhanced version of this model, named MAXBAND, was later developed by Little et al. (1981) to account for left-turn treatments and the impact of initial queues.

Grounded on the core logic of MAXBAND, Gartner et al. (1991) formulated a bandwidth optimization model, named MULTIBAND, to reflect the need of different bandwidths for links with different volumes. For the same purpose but with different formulations, Chaudhary et al. (2002) also developed a progression optimization program, named PASSER. To ensure the effectiveness of the optimized progression control, Tian and Urbanik (2007) developed a partition technique to facilitate the progression on the more important direction and keep sufficient green-band within the subsets of intersections. To account for the progression time uncertainty, Li (2014) proposed a set of formulations to assure the robustness of offsets for signal synchronization.

Besides those studies focused on the signal progression design at arterial level, some researchers also extended the models to grid networks. For example, Chang et al. (1988) implemented the MAXBAND model to a multi-arterial closed network and developed an optimization program, named MAXBAND-86. Similarly, another network version named MULTIBAND-96 was developed by Stamatiadis and Gartner (1996). However, such extensions may significantly increase the computation complexity due to the expanded size of integer variable set. To overcome this problem, Gartner and Stamatiadis (2002, 2004) proposed a two-step solution procedure that can improve the computing efficiency of existing progression models. Their proposed first step is to select a set of priority routes, each carrying a large volume, and then subsequently design signal progression for each selected priority route. The second step is to solve the progression optimization for the entire network by freezing the decision variables associated with each selected route. Following the same procedures to test each priority route in the set, one can compare its resulting objective function and then determine the optimal solution. Notably, this model was designed to generate green bands to traffic movements along those key routes rather than solely along the arterial. In design of signals for diverging diamond interchanges (DDI), Yang et al. (2014) proposed a progression model which can concurrently provide green bands to the off-ramp flows and local through traffic. However, since DDI are operated with simple two-phase signals, such a signal-progression model is only applicable for DDI's unique geometric features and limited intersections.

Existing studies in the second category focused mainly on minimizing the total delay for intersections within the control boundaries, where TRANSYT family (Robertson, 1969; Wallace et al., 1988), the simulation-based program, is the most commonly adopted tool by the traffic control community. With the similar simulation–optimization solution method, traffic researchers have also produced various models for design of arterial traffic signals. Examples of such studies include a set of mesoscopic optimizers by Yun and Park (2006) and Stevanovic et al. (2007); a GA-based method to identify cycle length, green splits, offsets, and phase sequences by Hadi and Wallace (1993) and Park et al. (1999).

In the same category of delay minimization but not using simulation, a variety of signal optimization is available in the literature (e.g., Aboudolas et al., 2010; Li, 2012). For example, to prevent intersection blockage, Liu and Chang (2011) proposed an optimization model to remove the blocking effects at local arterials. D'Ans and Gazis (1976) and Papageorgiou (1995) promoted the use of store-and-forward control models to perform real-time signal optimization. Kashani and Saridis (1983) offered a set of queue-and-dispersion models for arterial signal optimization. Yin (2008) and Yang et al. (2013) developed a robust optimization model to design pre-timed signal timings.

Note that all aforementioned studies, despite their significant contributions in traffic signal control, are mainly designed to minimize the delay or maximize the progression for through traffic flows over the arterial segment which is implicitly assumed to have the highest volume among all traffic movements. However, for commonly-observed arterials shown in Fig. 1, congestion patterns are caused by the turning volumes on some links. Under such condition, the design geared to best facilitate the through flows are likely to fall short of providing sufficient green times and proper offsets for those heavy path-flows which need to take several turning exercises along with through movement to move out of the target arterial segment. Hence, to prevent spillback or overflow on such arterials, one shall design the signal system based on the detected primary traffic-flow paths, and maximize the progression for not only the through traffic but all path-flows with significant volume.

In addition, due to the competing nature among all heavy-volume paths, an effective signal plan for arterial with multi-path flow patterns shall consider not only the optimized offsets for path flows, but also the optimal signal phase sequence at each intersection so that the competition of green bands between different paths can be minimized and the available green times can be fully utilized. This is quite different from the existing studies on arterial signal progression, where the primary decision variable is the set of offsets to maximize the progression bandwidth for through traffic flows. Grounded on the same notion as in Gartner and Stamatiadis (2002, 2004) and Yang et al. (2014), this paper presents three path-based progression models, proposed to account for multiple critical issues that need to be tackled in design of an effective progression system for congested arterials comprising complex traffic flow patterns. The proposed models have the following key features: (1) offering the green bandwidth along each traffic path, based on the phasing plans at both upstream and downstream intersections; (2) concurrently providing the phase sequence optimization at each intersection; and (3) accounting for the green-band competition between critical paths and identifying the optimal number of path-flows for progression operations.

2. Modeling methodology

In design of a new model to contend with multi-path arterial traffic patterns, this study starts with investigation of the fundamental two-way progression concept.

2.1. Two-way progression modeling concept

As noted in the literature, the pioneering work, MAXBAND, offers a rigorous method to concurrently generate the offsets between adjacent signals, optimize the prevailing speed at each link, and determine the proper left-turn phases. The key model variables in Little et al. (1981) are shown in Fig. 2, and their primary formulations are quoted below:

$$Max(b+k\bar{b}) \tag{1}$$

$$\text{s.t.}(1-\rho)\bar{b} \geqslant (1-\rho)\rho b \tag{2}$$

$$1/C_2 \leqslant z \leqslant 1/C_1 \tag{3}$$

$$w_i + b \leqslant 1 - r_i \quad \forall i = 1,\ldots,n \tag{4}$$

$$\bar{w}_i + \bar{b} \leqslant 1 - \bar{r}_i \quad \forall i = 1,\ldots,n \tag{5}$$

$$(w_i + \bar{w}_i) - (w_{i+1} + \bar{w}_{i+1}) + (t_i + \bar{t}_i) + \delta_i L_i - \bar{\delta}_i \bar{L}_i - m_i = (r_{i+1} - r_i) + (\tau_i + \bar{\tau}_i) + \delta_{i+1} L_{i+1} - \bar{\delta}_{i+1} \bar{L}_{i+1} \quad \forall i = 1,\ldots,n-1 \tag{6}$$

$$(d_i/f_i)z \leqslant t_i \leqslant (d_i/e_i)z \quad \forall i = 1,\ldots,n-1 \tag{7}$$

$$(\bar{d}_i/\bar{f}_i)z \leqslant \bar{t}_i \leqslant (\bar{d}_i/\bar{e}_i)z \quad \forall i = 1,\ldots,n-1 \tag{8}$$

$$(d_i/h_i)z \leqslant (d_i/d_{i+1})t_{i+1} - t_i \leqslant (d_i/g_i)z \quad \forall i = 1,\ldots,n-2 \tag{9}$$

$$(\bar{d}_i/\bar{h}_i)z \leqslant (\bar{d}_i/\bar{d}_{i+1})\bar{t}_{i+1} - \bar{t}_i \leqslant (\bar{d}_i/\bar{g}_i)z \quad \forall i = 1,\ldots,n-2 \tag{10}$$

$$b, \bar{b}, z, w_i, \bar{w}_i, t_i, \bar{t}_i \geqslant 0 \quad \forall i = 1,\ldots,n \tag{11}$$

$$m_i \text{ integer; } \delta_i, \bar{\delta}_i \text{ binary integers} \quad \forall i = 1,\ldots,n \tag{12}$$

Parameters included in above formulations are: r_i, the common red time at signal i; $L_i(\bar{L}_i)$, the time allocated to the left-turn movements; C_1 and C_2, the boundaries of the cycle length; $e_i, f_i(\bar{e}_i, \bar{f}_i)$, the lower and upper limits for the outbound (inbound) speeds; $g_i, h_i(\bar{g}_i, \bar{h}_i)$, the lower and upper limits for the outbound (inbound) speed change; ρ, the preference parameter.

Decision variables include: bandwidth $(b, \bar{b})$, cycle length (z), time between the start of a green phase and the boundary of its green band $(w_i, \bar{w}_i)$, prevailing speed $(t_i, \bar{t}_i)$, and integer variables $(\delta_i, \bar{\delta}_i, m_i)$. Particularly, different values of the binary variables, δ_i and $\bar{\delta}_i$, can result in four possible phase designs to accommodate major arterial flows: outbound left leads and inbound left lags; outbound left lags and inbound left leads; outbound (or inbound) left leads; and outbound (or inbound) left lags.

The objective function (1) for MAXBAND is to maximize the weighted sum of the two-way bandwidths. Constraint (2) allocates the progression preference to either the inbound or outbound direction. Constraint (3) limits the upper and lower bounds of the selected cycle length. The **directional interference constraints** in Eqs. ((4) and (5)) can ensure the green bandwidth to be within the available green time. The **loop integer constraint** in Eq. (6) is specified to guarantee that the signals will not cause traffic flows to stop in the green bands. The variation of travel times (a proxy of speed) is constrained by Eqs (7)–(10).

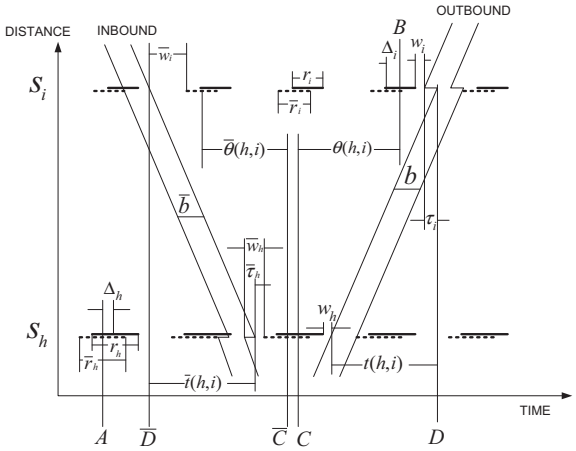

Fig. 2. Key notations in the MAXBAND model (Little et al., 1981).

2.2. Critical issues in a multi-path progression model

Based on the formulation of MAXBAND, one can note that such two-way progression model can only optimize the sequence of those phases dealing with major arterial flows. In contrast, any models designed for multi-path flows such as those comprising turning movements from/to side streets will certainly need a more advanced phase sequence optimization function.

For example, Fig. 3 shows an illustrative arterial that consists of three critical traffic paths. Aside from the through path (Path 1), turning flows along Path 2 will join the arterial via the side street at intersection-3 and traffic along Path 3 will leave the arterial to the side street at intersection-2. Given one phase sequence design, the green bandwidth along each path is presented in Fig. 3(a). However, after optimizing phase sequence at each intersection, the green bandwidths along all three paths increase significantly, as shown in Fig. 3(b). Based on this example, it is noticeable that a multi-path progression model shall account for both major arterial and cross street flows when optimizing phase sequences.

In addition to the phase sequence optimization, the loop integer constraint (Eq. (6)) in the MAXBAND which ensures that both through directions have non-zero bands (see Fig. 4(a)) also needs to be extended. This is due to the fact that such constraints in a multi-path progression system may result in near-zero or negligible bandwidths along some paths (see Fig. 4(b)). Furthermore, due to the competing nature of green bands, some path-flows may have to encounter the case shown in Fig. 4(c) and their loop integer constraints will not be satisfied. Under such conditions, the formulations for entire multi-path progression may yield an infeasible solution. Hence, extensions shall be made to overcome this problem in multi-path progression models.

In brief, an effective arterial signal model, grounded on the logic of MAXBAND, for multi-path progression needs to explicitly account for the following critical issues: (1) using a proper multi-phase plan for the path-based progression; (2) concurrently optimizing the signal phase sequence and offsets; and (3) effectively eliminating some infeasible path-flows so as to

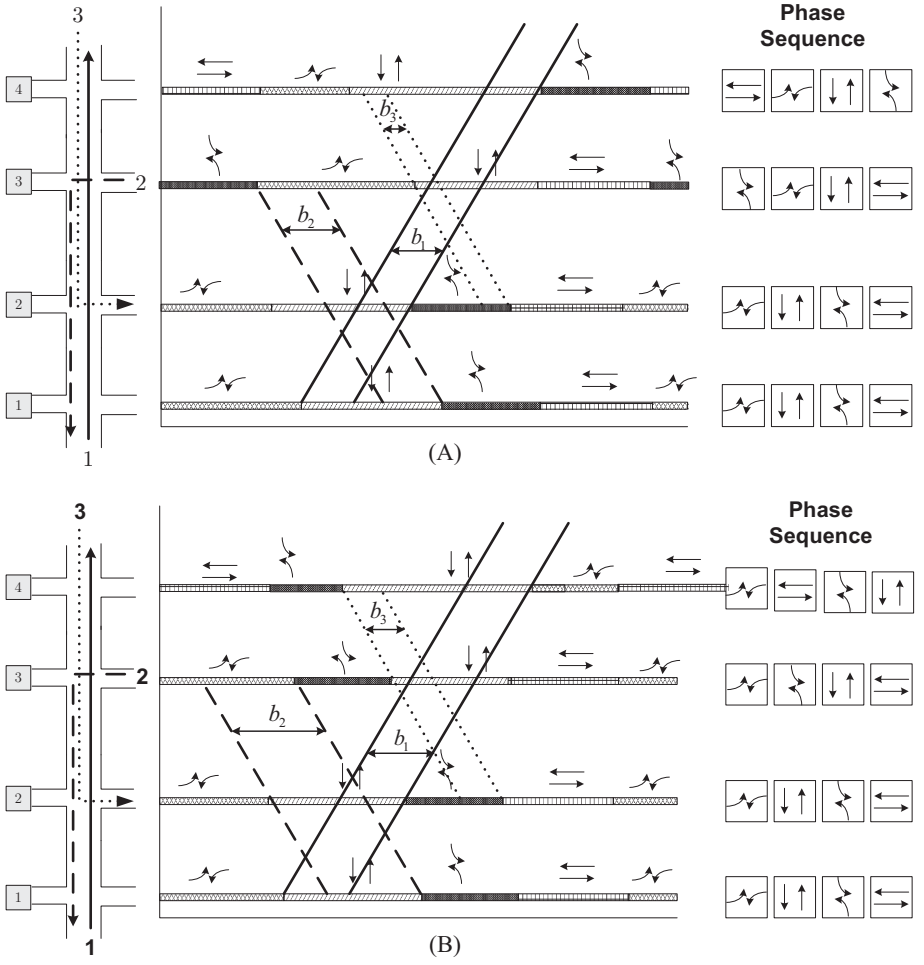

Fig. 3. An illustrative example for the multi-path progression.

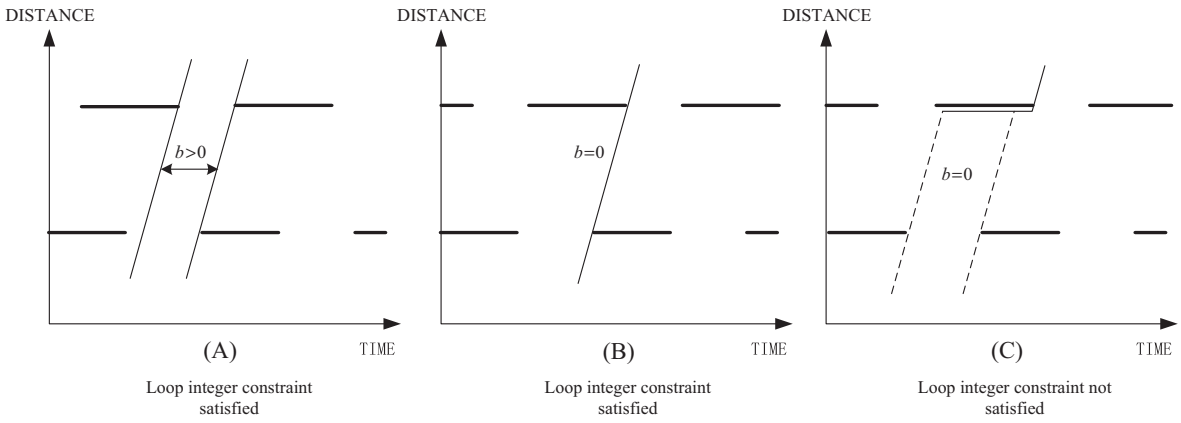

Fig. 4. Three possible cases for one particular progress path.

Table 1
Key notations.

Notation	Description
$\varphi_i(\overline{\varphi}_i)$	The weighting factor for the outbound (inbound) path i
$b_i(\bar{b}_i)$	The green bandwidth for outbound (inbound) path i
b_e	The effective green bandwidth in seconds
ξ	The reciprocal of cycle length
$g_{i,k}(\bar{g}_{i,k})$	The maximum green duration that the outbound (inbound) path i can obtain at intersection k
$w_{i,k}(\bar{w}_{i,k})$	The part of a green duration before (after) the green band for outbound (inbound) path i at intersection k
$\Omega(\overline{\Omega})$	The set of outbound (inbound) paths
σ_i	The set of intersections passed by path-flow i
θ_k	The offset of intersection k
$r_{i,k}$	The total red duration at the left side of the green band for path i
$\bar{r}_{i,k}$	The total red duration at the right side of the green band for path i
t_k	The travel time between intersection k and $k+1$
$\tau_{i,k}(\overline{\tau}_{i,k})$	The initial queue clearance time along path i at intersection k
$n_{i,k}(\bar{n}_{i,k})$	Integer variables to represent the number of signal cycles
$\phi_{l,k}$	The duration of phase l at intersection k
M	A large positive number
ρ	A parameter that can indicates the preference of inbound or outbound paths
$x_{i,j,k}$	Binary decision variable which represents the phase sequences at intersection k
$y_i(\bar{y}_i)$	Binary decision variable which indicates the selection of critical paths for progression

maximize the sum of weighted bandwidths for all identified paths, and to yield the maximal benefit for the total flows in the target arterial.

3. Model formulation

This section presents three sets of formulations, where the first is a direct-extension of MAXBAND for the multi-path scenario, and the second highlights the feature of concurrently optimizing phase sequences and offsets. An enhancement of the second model, designed to eliminate the likelihood of generating some non-productive progression bands, will also be discussed. Note that the non-productive band is defined in this study as the bandwidth that is not sufficient to accommodate a prespecified number of vehicles (e.g., 3 vehicles). Key notations in these three proposed models are shown in Table 1 and Fig. 5.

3.1. Model I: optimize offsets only for all target path flows

As discussed previously, with the identified multi-path traffic flow patterns, phase plans, and sequences, one can directly extend MAXBAND with the following objective function for offset optimization:

$$Max \sum_i (\varphi_i b_i) + \sum_i (\overline{\varphi}_i \bar{b}_i) \tag{13}$$

Similar to MAXBAND, the interference constraints for a multi-path progression system are given as follows

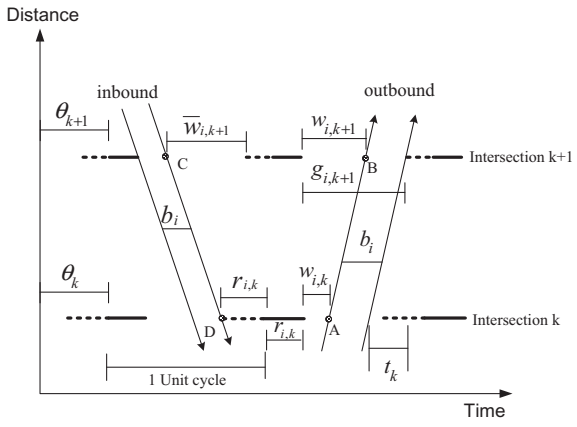

Fig. 5. Key notations in the proposed models.

$$0 \leqslant w_{i,k} + b_i \leqslant g_{i,k} \quad \forall i \in \Omega;\ \forall k \in \sigma_i \tag{14}$$

$$0 \leqslant \bar{w}_{i,k} + \bar{b}_i \leqslant \bar{g}_{i,k} \quad \forall i \in \overline{\Omega};\ \forall k \in \sigma_i \tag{15}$$

Note that the formulations for MAXBAND are based on a signal plan for two-way progression. Hence, the loop integer constraint (Eq. (6)) can be obtained by substituting those two progression constraints for inbound and outbound through paths. However, due to the complexity of the multi-path progression nature, one shall explore new constraints to represent the progress of green bands for all identified path flows, rather than directly using the same loop integer constraints in MAXBAND. In this study, a set of alternative progression constraints are derived to represent the progress of an outbound green band from point A to point B (see Fig. 5):

$$\theta_k + r_{i,k} + w_{i,k} + t_k + n_{i,k} = \theta_{k+1} + r_{i,k+1} + w_{i,k+1} + \tau_{i,k+1} + n_{i,k+1} \quad \forall i \in \Omega;\ \forall k \in \sigma_i \tag{16}$$

Similarly, for traffic along the inbound paths, one can use the following equation to represent the progress of the green band from point C to point D as shown in Fig. 5:

$$-\theta_k + \bar{r}_{i,k} + \bar{w}_{i,k} - \overline{\tau}_{i,k} + \bar{t}_k + \bar{n}_{i,k} = -\theta_{k+1} + \bar{r}_{i,k+1} + \bar{w}_{i,k+1} + \bar{n}_{i,k+1} \quad \forall i \in \overline{\Omega};\ \forall k \in \sigma_i \tag{17}$$

Given the green durations for all intersections, one can then compute the value of $r_{i,k}(\bar{r}_{i,k})$ and $g_{i,k}(\bar{g}_{i,k})$ with the pre-determined phase sequences. Hence, the Model I (M1) could be summarized as follows:

$$\text{M1}: Max \sum_i (\varphi_i b_i) + \sum_i (\overline{\varphi}_i \bar{b}_i)$$

s.t. Eqs.(14)—(17)

$$b_i, w_{i,k},\ \bar{b}_i, \bar{w}_{i,k} \geqslant 0 \quad \forall i \in \Omega + \overline{\Omega};\ \forall k \in \sigma_i$$

$n_{i,k}, \bar{n}_{i,k}$ are integer variables

Note that the M1 model assumes that the travel speeds on all links are predetermined. To concurrently optimize the progression speeds, one can simply add additional constraints shown in Eqs. ((7)–(10)).

3.2. Model II: Concurrently optimize phase sequences and offsets

As shown in Fig. 2, changing phase sequence at each intersection can minimize the green band competition between different path flows. To optimize such sequences, one can first define a set of binary variables as follows:

$$x_{l,m,k} = \begin{cases} 1, & \text{if phase } l \text{ is before phase } m \text{ within the same cycle of intersection } k; \\ 0, & \text{o.w.} \end{cases} \tag{18}$$

To ensure the operational feasibility of each produced phase sequence, this study has further specified the following constraints related to $x_{l,m,k}$:

$$x_{l,l,k} = 0 \quad \forall l;\ \forall k \tag{19}$$

$$x_{l,m,k} + x_{m,l,k} = 1 \quad \forall l \neq m;\ \forall k \tag{20}$$

$$x_{l,n,k} \geqslant x_{l,m,k} + x_{m,n,k} - 1 \quad \forall l \neq m \neq n;\ \forall k \tag{21}$$

$$x_{l,n,k} + x_{n,m,k} = 1 \quad l \neq m \neq n \tag{22}$$

$$x_{l,m,k} = 1 \quad l \neq m \tag{23}$$

$$x_{l,m,k} - x_{l',m',k+1} = 0 \quad \forall k \tag{24}$$

Note that Eq. (20) is based on the definition of $x_{l,m,k}$ and Eq. (20) indicates that phase l is either before or after phase m. To prevent a "sub-loop" in a phase sequence, the model must ensure that "if phase l is before phase m ($x_{l,m,k} = 1$) and phase m is before phase n ($x_{m,n,k} = 1$), then phase l is before phase n ($x_{l,n,k} = 1$)". The mathematical formulations are shown in Eq. (21) for such relations. Eqs. ((22)–(24)) are three optional constraints. Eq. (22) ensures that phase l and m in a sequential order. Eq. (23) indicates that phase l is ahead of phase m, and Eq. (24) is functioned to guarantee the consistence of phase sequence designs between adjacent intersections.

To describe the relations between signal phases and path-flows, one can further define a set of binary parameters as follows:

$$\beta_{i,l,k} = \begin{cases} 1, & \text{if path } i \text{ obtains green in phase } l \text{ at intersection } k; \\ 0, & \text{o.w.} \end{cases} \tag{25}$$

Hence, one can compute the available green duration for the progress of an outbound (inbound) path i, $g_{i,k}(\bar{g}_{i,k})$ with the following equations:

$$g_{i,k} = \beta_{i,l,k}\phi_{l,k} \quad \forall i \in \Omega;\ \forall k \in \sigma_i \tag{26}$$

$$\bar{g}_{i,k} = \beta_{i,l,k}\phi_{l,k} \quad \forall i \in \Omega;\ \forall k \in \sigma_i \tag{27}$$

Then, the interference constraints can be re-written as follows:

$$0 \leqslant w_{i,k} + b_i \leqslant \sum_l \beta_{i,l,k}\phi_{l,k} \quad \forall i \in \Omega;\ \forall k \in \sigma_i \tag{28}$$

$$0 \leqslant \bar{w}_{i,k} + \bar{b}_i \leqslant \sum_l \beta_{i,l,k}\phi_{l,k} \quad \forall i \in \overline{\Omega};\ \forall k \in \sigma_i \tag{29}$$

Note that in M1 model, the red duration of path i before (after) its available green time, $r_{i,k}(\bar{r}_{i,k})$, can be directly computed since the phase sequences are provided. However, by relaxing the phase sequences as decision variables, the values of $r_{i,k}(\bar{r}_{i,k})$ will be varied with the selected phase sequence. Hence, to ensure the progression constraints to function properly as shown in Eqs. ((16) and (17)), one shall establish the relations between phase sequences, $x_{l,m,k}$, and red durations $r_{i,k}(\bar{r}_{i,k})$. A set of constraints for such a need are given below:

$$r_{i,k} \leqslant \sum_l \beta_{i,m,k} x_{l,m,k} \cdot \phi_{l,k} + M(1 - \beta_{i,m,k}) \quad \forall i \in \Omega + \overline{\Omega}; \forall k \in \sigma_i;\ \forall m \tag{30}$$

$$\bar{r}_{i,k} \leqslant \sum_l \beta_{i,m,k} x_{m,l,k} \cdot \phi_{l,k} + M(1 - \beta_{i,m,k}) \quad \forall i \in \Omega + \overline{\Omega};\ \forall k \in \sigma_i; \forall m \tag{31}$$

$$r_{i,k} + \bar{r}_{i,k} + \sum_l \beta_{i,l,k} \cdot \phi_{k,n} = 1 \quad \forall i \in \Omega + \overline{\Omega};\ \forall k \in \sigma_i \tag{32}$$

where M is a large positive number. The second term at the right side of Eq. (30) is used to dominate other variables when path i cannot receive green in phase m ($\beta_{i,m,k} = 0$). If path i can receive green in phase m ($\beta_{i,m,k} = 1$), the first term in Eq. (30) will function to compute the time duration before phase m. Following the similar logic, the first term in the right side of Eq. (31) is used to compute the duration after phase m if $\beta_{i,m,k} = 1$. Since path i may receive green in multiple consecutive phases, Eqs. ((30) and (31)) will ensure that $r_{i,k}(\bar{r}_{i,k})$ is taking place prior (after) the first (last) phase that is given green to path i. Also note that the third term in Eq. (32) is the total green duration that path i can obtain within one cycle. Hence, Eqs. ((30)–(32)) together can force $r_{i,k}(\bar{r}_{i,k})$ to equal the red duration before (after) the green time of path i, which corresponds to its definition. A detailed explanation of constraints (30)–(32) is given in the Appendix-A.

In brief, the M2 model could be summarized as follows:

$$\text{M1}: Max \sum_i (\varphi_i b_i) + \sum_i (\overline{\varphi}_i \bar{b}_i)$$

s.t. Eqs. (16) and (17)

Eqs. (19)—(24)

Eqs. (28)—(32)

$b_i, w_{i,k},\ \bar{b}_i, \bar{w}_{i,k} > 0 \quad \forall i \in \Omega + \overline{\Omega};\ \forall k \in \sigma_i$

$n_{i,k}, \bar{n}_{i,k}, x_{i,j,k}$ are integer variables

3.3. Model III: Select part of paths for progression and prevent infeasible solutions

Note that both the M1 and M2 models assume that every selected critical path can receive a green band on the arterial, regardless of the fact that some bandwidths may be close to zero. In other words, the progression constraints (16) and (17) will ensure that every selected path can obtain a bandwidth under the conditions in either Fig. 4(a) or (b). Obviously,

providing a near-zero green band is practically non-productive, and removing the constraints of those paths may offer a larger bandwidth to other primary paths. Also, with an increase in the number of paths and intersections, some paths may inevitably encounter the case in Fig. 4(c), due to their competing for progression. Consequently, both the M1 and M2 models will yield no feasible solutions under such condition.

To tackle such issues, we have further defined a set of new decision variables to automatically select proper paths for green-band maximization in M3 model:

$$y_i(\bar{y}_i) = \begin{cases} 1, & \text{if path } i \text{ obtains signal progression with non} - \text{zero green band} \\ 0, & \text{o.w,} \end{cases} \tag{33}$$

Then, the following additional constraints are derived to remove those paths without progression from the optimization process:

$$b_i \leqslant y_i \tag{34}$$

$$\bar{b}_i \leqslant \bar{y}_i \tag{35}$$

$$b_i \geqslant b_e\xi - M(y_i - 1) \tag{36}$$

$$\bar{b}_i \geqslant b_e\xi - M(\bar{y}_i - 1) \tag{37}$$

Note that Eqs. ((34) and (35)) are used to force the bandwidth of path i to zero if it is removed from progression need ($y_i = 0$) and Eqs. ((36) and (37)) are functioned to guarantee the minimum effective bandwidth is satisfied.

For those outbound paths without progression, one needs to relax their corresponding progression constraints to ensure the feasibility of the optimization model. To do so, one can rewrite the set of progression constraints in Eq. (16) as follows:

$$\theta_k + r_{i,k} + w_{i,k} + t_k + n_{i,k} \geqslant \theta_{k+1} + r_{i,k+1} + w_{i,k+1} + \tau_{i,k+1} + n_{i,k+1} - M(1 - y_i)\ \forall i \in \Omega;\ \forall k \in \sigma_i \tag{38}$$

$$\theta_k + r_{i,k} + w_{i,k} + t_k + n_{i,k} \leqslant \theta_{k+1} + r_{i,k+1} + w_{i,k+1} + \tau_{i,k+1} + n_{i,k+1} + M(1 - y_i)\ \forall i \in \Omega;\ \forall k \in \sigma_i \tag{39}$$

Since M can dominate any variable in the constraints, Eqs. ((38) and (39)) will become ineffective when y_i equals zero.

Grounded on the same logic, one can derive the following constraints for the inbound paths by modifying Eq. (17) as follows:

$$-\theta_k + \bar{r}_{i,k} + \bar{w}_{i,k} - \bar{\tau}_{i,k} + \bar{t}_k + \bar{n}_{i,k} \geqslant -\theta_{k+1} + \bar{r}_{i,k+1} + \bar{w}_{i,k+1} + \bar{n}_{i,k+1} - M(1 - \bar{y}_i)\ \forall i \in \overline{\Omega};\ \forall k \in \sigma_i \tag{40}$$

$$-\theta_k + \bar{r}_{i,k} + \bar{w}_{i,k} - \bar{\tau}_{i,k} + \bar{t}_k + \bar{n}_{i,k} \leqslant -\theta_{k+1} + \bar{r}_{i,k+1} + \bar{w}_{i,k+1} + \bar{n}_{i,k+1} + M(1 - \bar{y}_i)\ \forall i \in \overline{\Omega};\ \forall k \in \sigma_i \tag{41}$$

Note that under some extreme scenarios, the enhanced model may sacrifice all paths from one direction (e.g. inbound) and offers only a one-direction progression if they are specified with larger weighting factors. Hence, similar to the constraint (2) in MAXBAND, the following constraint should be satisfied:

$$(1 - \rho)\sum_{i \in \overline{\Omega}} \bar{b}_i \geqslant (1 - \rho)\rho \sum_{i \in \Omega} b_i \tag{42}$$

In brief, the model III (M3) could be summarized as follows:

$$\text{M3}: \ Max \sum_i (\varphi_i b_i) + \sum_i (\overline{\varphi}_i \bar{b}_i)$$

s.t. Eqs. (19)—(24)

Eqs. (28)—(32)

Eqs. (34)—(42)

$b_i, w_{i,k},\ \bar{b}_i, \bar{w}_{i,k} \geqslant 0\ \forall i \in \Omega + \overline{\Omega};\ \forall k \in \sigma_i$

$n_{i,k}, \bar{n}_{i,k}, x_{i,j,k},\ y_i, \bar{y}_i$ are integer variables

Note that all above three models, M1, M2 and M3, are formulated as mixed-integer-linear-programming problems, which can be solved with existing algorithms such as Branch-and-Bound.

4. Numerical examples

In this section, all mixed-integer-linear-programming problems are solved in Lingo 6.0 which is operated on a PC with 3 GHz CPU, 4 GB RAM, and Windows 7 operating system.

4.1. Case study 1

The test network used to evaluate the proposed models consists of an arterial of six intersections. As shown in Fig. 6, six critical paths have been identified along the arterial, where Paths 1, 2, and 3 are for outbound flows and the remaining paths are for inbound flows.

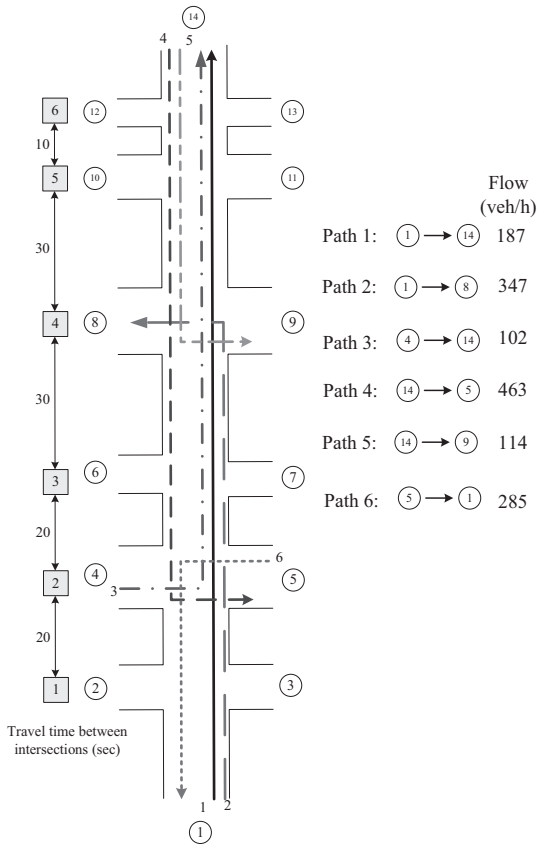

Fig. 6. Illustration of the test arterial.

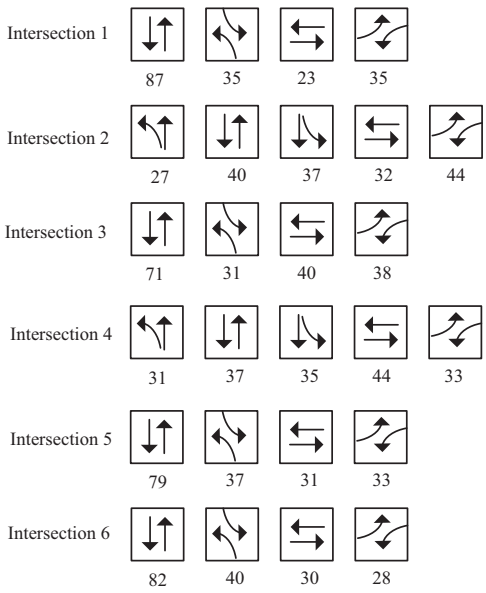

Fig. 7. Signal timings and the initial phase sequences.

The phasing plan, signal timings, and original phase sequence at each intersection are presented in Fig. 7. The common cycle length is set to be 180 s. The weighting factors for the six paths are set as 0.2, 0.4, 0.1, 0.5, 0.1, and 0.3, respectively.

Using the signal plans shown in Fig. 7 and assuming no initial queues on all links, the first model, M1, is implemented to optimize the offset at each intersection. The resulting green bandwidth for each path is presented in Fig. 8, where paths 5 and

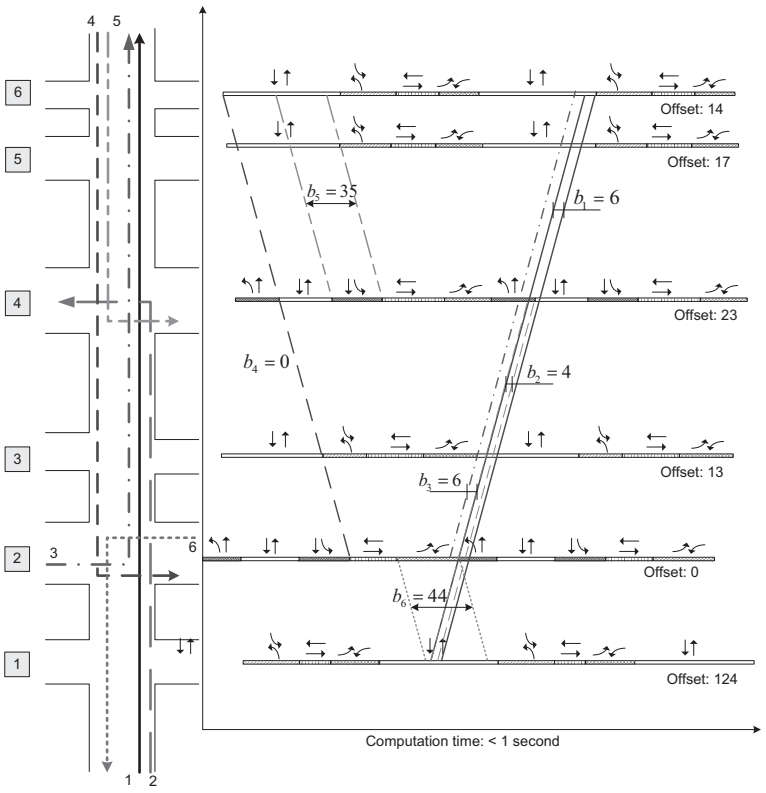

Fig. 8. The resulting green bands obtained by Model I.

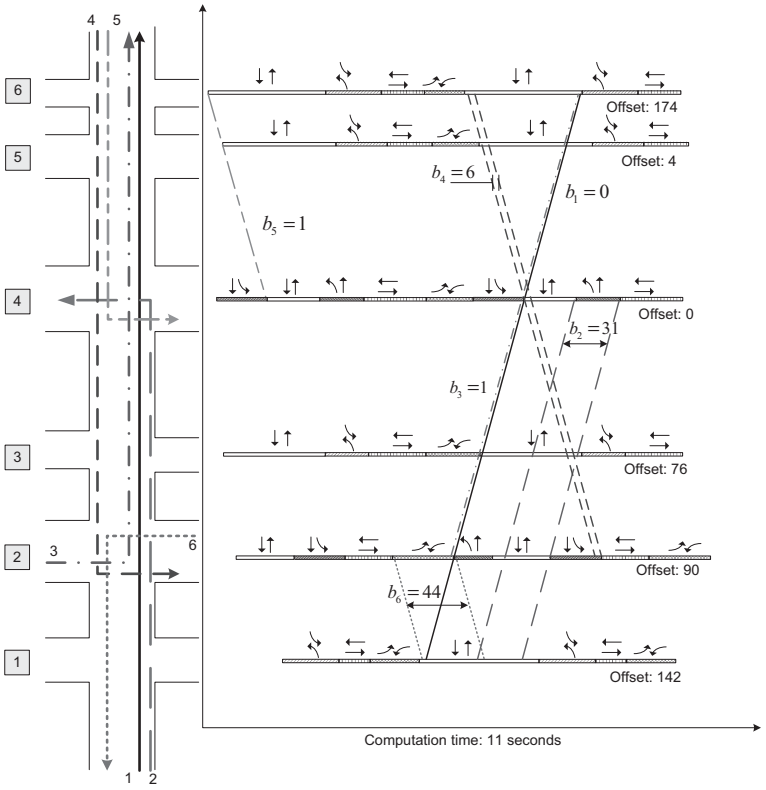

Fig. 9. The resulting green bands obtained by Model II.

6 have relatively wider green bands than those for Paths 1–4. Notably, the bandwidth for path 4 is zero and its green band is actually converged into a single line. The sum of all weighted bandwidths for this signal plan is 20.1 s.

By specifying the phase sequence at each intersection as a decision variable, Fig. 9 shows the resulting signal plan obtained by M2 model. Comparing with the results from M1 model, the bandwidth for Paths 1, 3 and 5 are nearly reduced to zeroes and the bandwidth of Path 6 remains unchanged. The bandwidths for Paths 1 and 4 have been increased. The sum of weighted bandwidths for this signal plan is 28.8 s, which is larger than the one produced by M1 model.

From both Figs. 8 and 9, one can observe that the bandwidths of several paths are close to zeroes, which are not useful in practice. Moreover, incorporating the progression constraints of those paths in the optimization models will reduce the feasible solution set which will in turn impact the progression results of the remaining paths. The results from the M3 model, designed to circumvent the limitations of the M1 and M2 models, are shown in Fig. 10, whose five out of six paths are concurrently accounted for progression and no near-zero green bands are found in this case. Due to competing with other paths, Path 3 has been automatically removed from progression and its corresponding constraints have become ineffective during the solution process. The sum of weighted bandwidths for this signal plan is 50.7, which is much larger than the results from the M1 and M2 models.

To further compare the operational performances of the target arterial under the control of these three models, this study has further implemented VISSIM for evaluations. Based on the simulation results summarized in Table 2, one can conclude that the M3 model with additional critical constraints can outperform the other two models in reducing average path-flow delay, average number of stops and improving average travel speed.

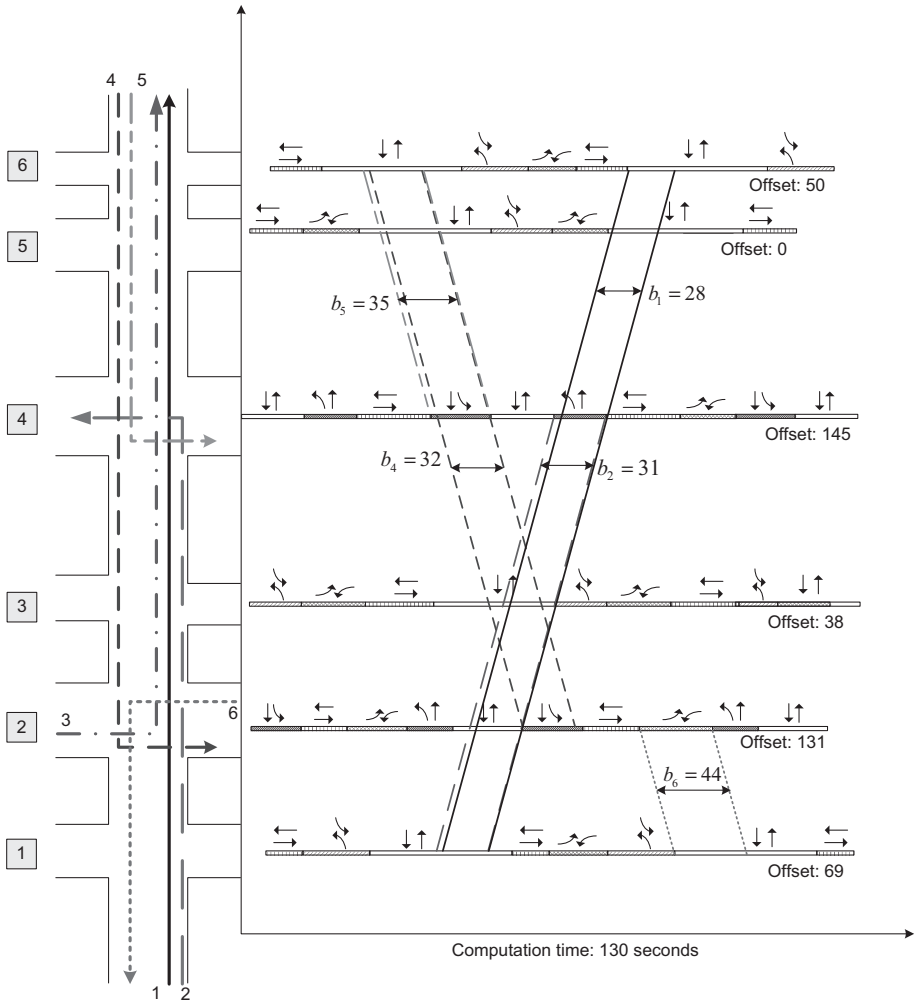

Fig. 10. The resulting green bands obtained by Model III. (For interpretation of the references to colour in this figure legend, the reader is referred to the web version of this article.)

Table 2
Arterial performance under the control of different models.

MOEs	M1 model	M2 model	M3 model
Average path-flow delay	45.2 s	41.8 s	37.5 s
Average # of stops	0.981	0.967	0.895
Average speed	34.7 km/h	36.4 km/h	40.3 km/h

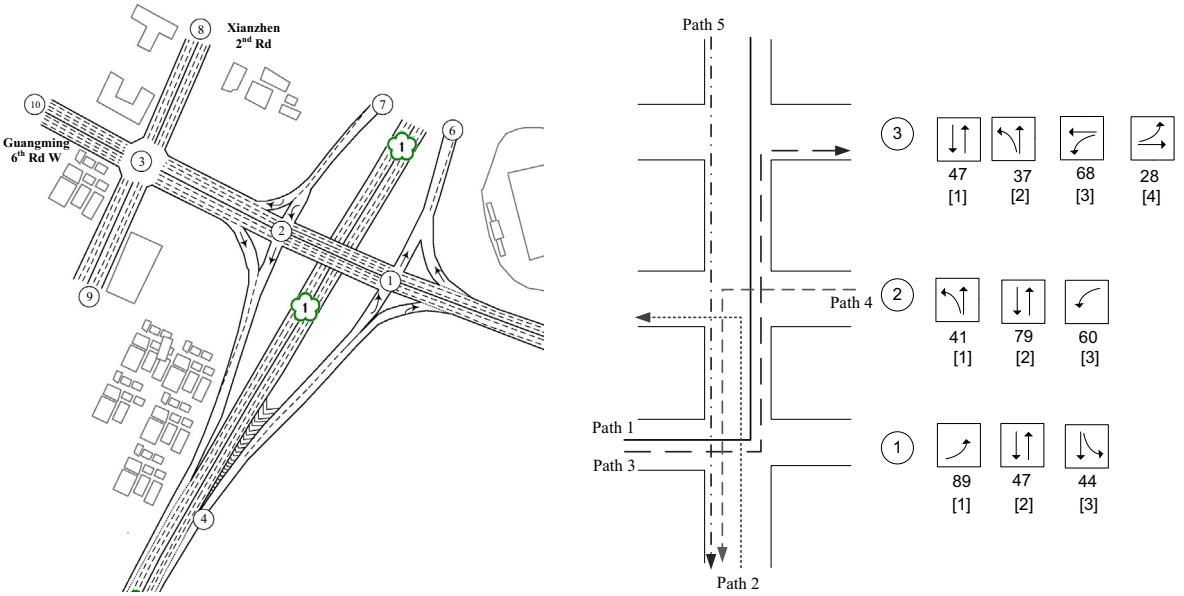

(A) The geometric layout of the study site (B) Critical paths and signal timings

Fig. 11. The general information of the study site.

4.2. Case study 2

To evaluate the potential of the proposed models for real-world applications, this study has further selected an arterial segment of three intersections in Chupei, Taiwan for case study. As shown in Fig. 11(a), during PM peak hours, heavy traffic flows will take the off-ramp to enter the Guanming 6th Rd, which constitutes several turning paths of heavy volumes on the arterial along with the local through traffic.

To analyze the demand patterns at the study site, the research team at the National Chiao Tung University (NCTU) in a project sponsored by Ministry of Communications and Transportation, has completed a field survey from 16:30 to 21:30 on April 24, 2013. Based on the collected data, they also performed an OD estimations and supplemental surveys on the target arterial segment, and identified five critical paths (see Fig. 11(b)). Table 3 presents the demand patterns at each intersection for the case study.

As shown in the previous section, since the M3 model can outperform the other two models, this field study has tested only this model. Based on the volumes along those five paths, the following factors, 0.5, 0.4, 0.3, 0.3, and 0.1, are set for the maximization of progress bands. Also, for comparison, the progression plans generated by the following three models are adopted in this study:

- MAXBAND-1: a two-way progression model designed for traffic along local arterials (Little et al., 1981).
- MAXBAND-2: a two-way progression model designed for traffic along the major route flows (i.e., Path-1 and Path 5).
- TRANSYT 7-F: an optimization model with the objective of minimizing the pre-defined performance Index (e.g., delay, number of stops).

Table 4 and Fig. 12 reports the signal plans obtained from all tested models. The cycle length in all plans is set to be 180 s; the initial phase sequence, phasing designs, and green times are shown in Fig. 11(b). Note that the shifts of green bands in Fig. 12 caused by the impact of initial queues. Similar to the MAXBAND model, the initial queue clearance time $\tau_{i,k}(\bar{\tau}_{i,k})$ are estimated with those uncoordinated flows.

To evaluate the network performance produced by different optimization models, this study selected VISSIM as the simulation platform. Recognizing that a simulated system is meaningful only if it can faithfully reflect actual traffic patterns,

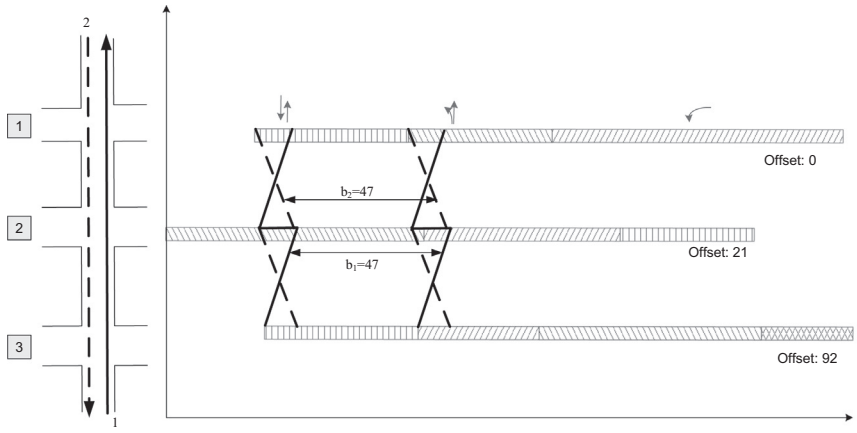

(A) Green bands by MAXBAND-1

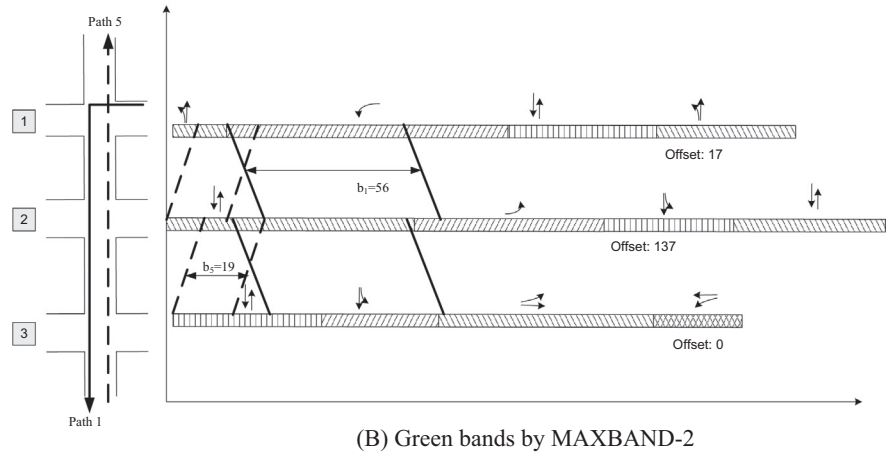

(B) Green bands by MAXBAND-2

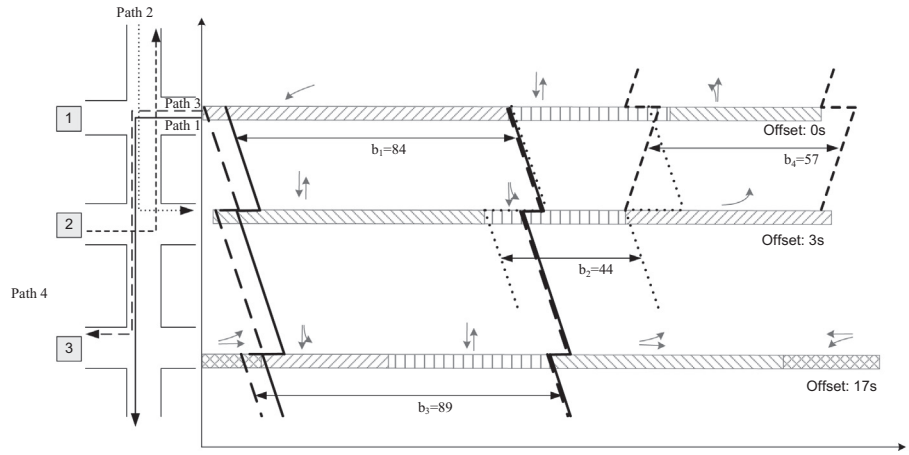

(C) Green bands by M3 for multiple critical traffic paths

Fig. 12. The resulting green bands obtained by different models.

this study has performed the calibration by minimizing the differences between simulated and field-collected queues and flow rates.

Based on the simulation results, Fig. 13 presents the time-dependent travel time distribution along each critical path. Compared with the plans from MAXBAND-1, MAXBAND-2 and TRANSYT 7-F, the proposed M3 model can produce much lower travel time along Path 1, as evidenced by the results in Fig. 13a. This is due to the fact that the movement along Path

Table 3
The three-hour demand patterns for the three intersections.

Time	Intersection	Westbound			Northbound			Eastbound			Southbound		
		L	T	R	L	T	R	L	T	R	L	T	R
17:00–18:00	1	/	924	/	1090	/	1073	518	976	/	/	/	/
	2	508	1506	/	/	/	/	/	907	/	587	/	672
	3	332	1056	790	/	274	451	82	834	91	729	272	74
18:00–19:00	1	/	786	/	1050	/	1011	441	968	/	/	/	/
	2	418	1418	/	/	/	/	/	857	/	551	/	729
	3	363	962	822	/	288	371	88	832	86	761	354	64
19:00–20:00	1	/	665	/	995	/	968	443	840	/	/	/	/
	2	269	1391	/	/	/	/	/	921	/	362	/	403
	3	287	872	635	/	238	300	82	653	91	658	286	69

Table 4
The resulting signal plans by different models.

Model	Intersection 1		Intersection 2		Intersection 3	
	Phase sequence	Offset (s)	Phase sequence	Offset (s)	Phase sequence	Offset (s)
MAXBAND-1	[1] [2] [3]	0	[1] [2] [3]	21	[1] [2] [3]	92
MAXBAND-2	[1] [2] [3]	17	[1] [2] [3]	137	[1] [2] [3]	0
7-F	[1] [3] [2]	14	[1] [2] [3]	157	[1] [2] [3] [4]	34
M3	[1] [3] [2]	0	[2] [1] [3]	3	[2] [1] [3] [4]	17

Note: the IDs of the phases are shown in Fig. 11(B).

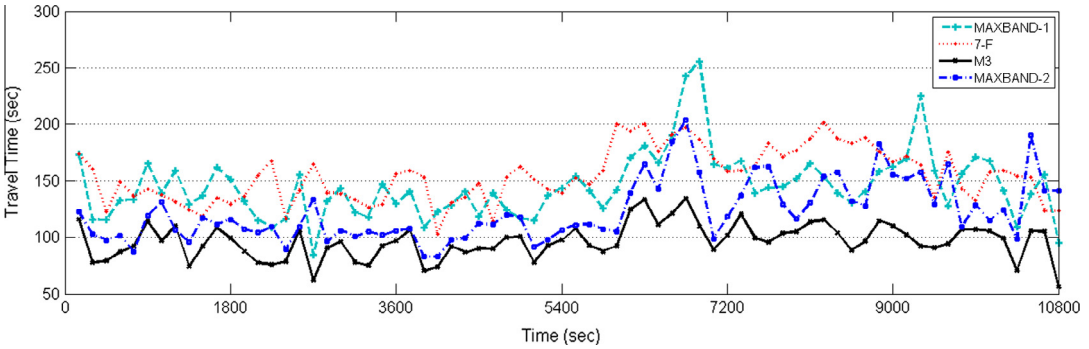

Fig. 13a. The time-dependent travel time along Path 1.

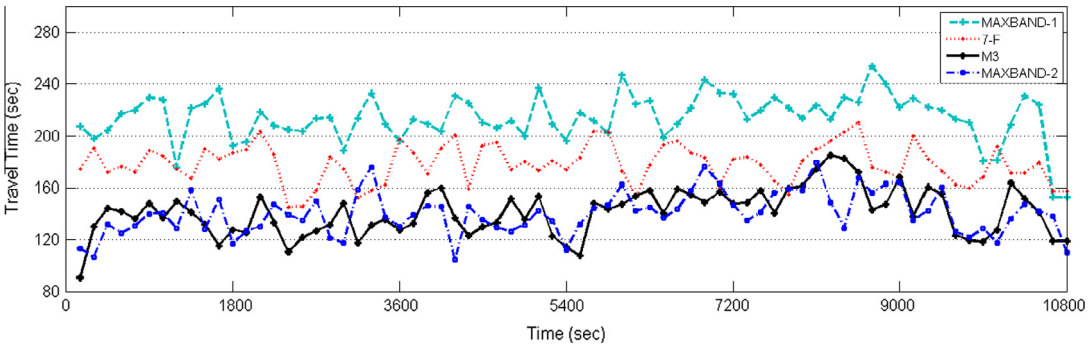

Fig. 13b. The time-dependent travel time along Path 2.

1 has the largest weighting factor in the M3 model and thus receives the progression priority. Also, MAXBAND-2 can outperform MAXBAND-1 since it takes Path-1 as the outbound route for designing progression. The travel times produced by TRANSYT 7-F are higher than those by the two MAXBAND models.

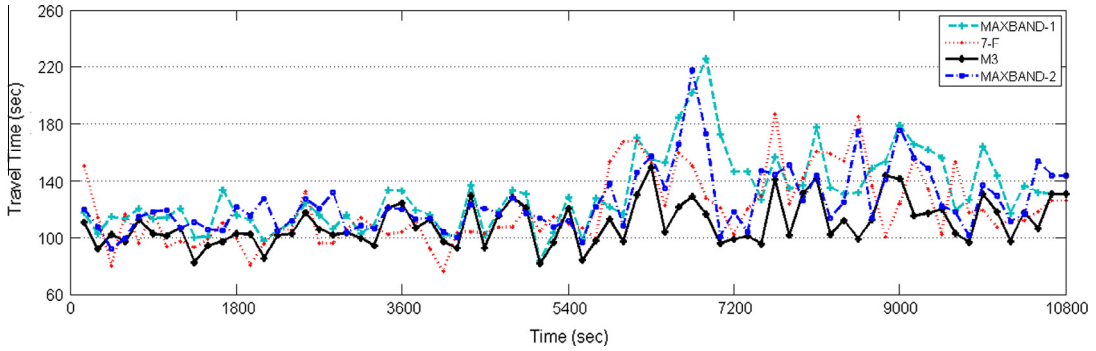

Fig. 13c. The time-dependent travel time along Path 3.

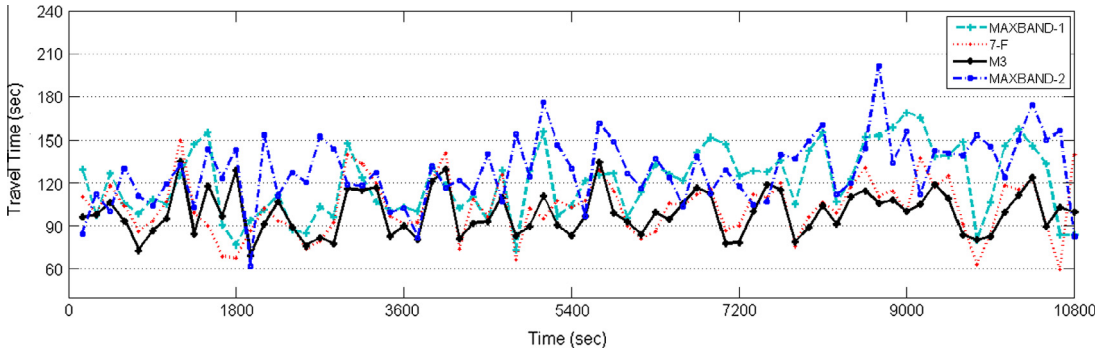

Fig. 13d. The time-dependent travel time along Path 4.

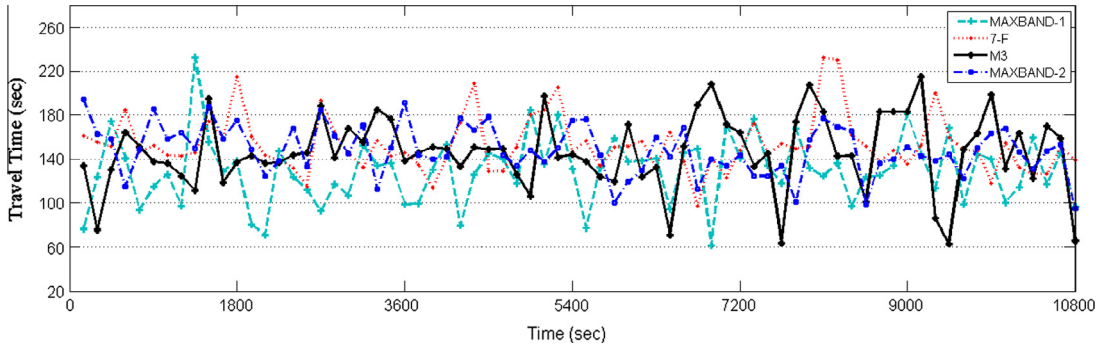

Fig. 13e. The time-dependent travel time along Path 5.

Fig. 13b shows the comparison of travel time for Path 2. Obviously, the other three models outperform MAXBAND-1 with respect to this path. Based on the trajectory of Path 2, one can observe that vehicles will make left-turns at the second intersection and then leave the arterial. Notably, with the MAXBAND-1 model, the green bands are assigned to the through paths only, so vehicles along Path 2 would consequently experience higher delays. However, in MAXBAND-2, traffic along Path 2 can occasionally receive a certain green band even though it is not accounted for in the model.

As shown in both Figs. 13c and 13d, the M3 model can also outperform the other three models since it has also offered green bands to Path 3 and Path 4. An interesting observation revealed in Fig. 13e is that the travel time differences along Path 5 by different models are not significant, while MAXBAND-1 model has produced a much wider green band along this path than with the other three models. By analyzing the simulation results, we have observed that most traffic volumes along Path 5 have only utilized half of the green band due to its low flow rate. Hence, the provided green band by MAXBAND-1 model has exceeded the need of traffic volume along Path 5, which results in the insignificant improvement of travel time as shown in Fig. 13e.

Table 5
Arterial performance under the control of different models.

MOEs	MAXBAND-1	MAXBAND-2	TRANSYT 7-F	M3 model
Average delay	54.3 s	50.1 s	55.4 s	47.6 s
Average # of stops	0.972	0.936	1.047	0.884
Average speed	34.7 km/h	35.4 km/h	31.3 km/h	40.5 km/h

In conclusion, the proposed M3 model, as expected, can efficiently produce progress bands and less travel times for vehicles along all identified critical paths. To further evaluate the progression-based signal plan over the entire network with different MOEs, Table 5 summarizes the resulting average delays, average number of stops, and average speeds. Notably, the proposed M3 model can produce the lowest delay compared with the other three models. The same trend could be found for the average number of stops. Regarding the average speed, the M3 model can also yield significant improvement. In brief, the proposed M3 model has the promising property of producing progression bands to arterials with heavy flow rates on multiple paths, and the resulting signal plan can also achieve the control objective of minimizing vehicle delays and stops. MAXBAND-2 can outperform MAXBAND-1 since it generated green bands to traffic movements along the key routes rather than solely along the arterial.

5. Conclusions

Existing models or tools for arterial signal control, focusing either on maximizing the progression for two-way through traffic flows or minimizing their total delay, cannot adequately account for some heavy-path flows that need to take multiple turning movements along the arterial. Hence, providing the progression for not only the through traffic but also other paths of heavy flows is essential in tackling the congestion causing by the overflows from turning bays or link blockage due to spill-back in many congested commuting arterials.

This paper has presented a multi-path progression model to concurrently optimize the phase sequence at each intersection and the progression bands for some identified critical path-flows that constitute the complex traffic pattern in congested urban arterials serving mainly as connectors between freeway traffic and surface-street flows. Different from the use of only intersection traffic counts, the proposed model can take full advantage of identified path-flow information in each congested link, and offer the progression for vehicles along each O-D path under the optimized phase sequence. Due to the competing nature among identified path flows, the proposed model can further identify the set of productive progression paths, based on the distribution of link volumes over each O-D path, and yield the optimal number of progression paths and bandwidths for the target arterial.

The results of extensive numerical investigation with field data have confirmed that the proposed model clearly outperforms the conventional design methods, such as with MAXBAND or TRANSYT, especially for those arterials where heavy path-flows from-and-to the freeway travel over only some of the arterial links but need to execute both left and right turns from the available short turning bays. The research results from this study has also reflected the need to collect more traffic pattern data such as major path-flow volumes, in addition to the typical intersection volume counts, in design of signal plans for arterials suffering from heavy turning flows and their maneuvers between turning bays and travel lanes.

Further extensions along this line will be focused on advancing the proposed models to integrate with real-time local adaptive control. The purpose is to ensure that the computed offsets and bandwidths can precisely accommodate the needs of all real-time arriving path flows which may fluctuate from day to day.

Acknowledgments

The authors are grateful for the data provided by the National Chiao Tung University for its project sponsored by Taiwan Ministry of Communications and Transportation. The simulation calibration work done by Yang (Carl) Lu at the University of Maryland is also appreciated.

Appendix A

Considering a signal cycle with N phases at intersection k, one critical path i can receive the green within the phases $[p_e, p_{e+s}]$. Here $\{p_e\}$ refers to the index of one particular phase at intersection k, thus its value may fall between $[1, N]$ and:

$$p_i \neq p_j \ \forall \ i \neq j \tag{A1}$$

Hence, different combination patterns of $\{p_e\}$ can represent different phase sequences.

Proof the effectiveness of constraints (27)–(29)

Given the constraint (27):

$$r_{i,k} \leqslant \sum_l \beta_{i,m,k} x_{l,m} \phi_{l,k} + M(1 - \beta_{i,m,k}) \quad \forall i \in \Omega + \overline{\Omega};\ \forall k \in \sigma_i;\ \forall m \tag{27}$$

Fig. A1. (a) The phase diagram at intersection k.

For the case shown in Fig. A1, it can give:

$$r_{i,k} \leqslant \sum_{l} 0 \cdot x_{l,m} \cdot \phi_{l,k} + M(1-0) = M \quad \forall p_m \in [p_1, p_{e-1}] \tag{A2}$$

$$r_{i,k} \leqslant \sum_{l=p_1}^{p_{m-1}} 1 \cdot 1 \cdot \phi_{l,k} + \sum_{p_m}^{p_N} 1 \cdot 0 \cdot \phi_{l,k} + M(1-1) = \sum_{l=p_1}^{p_{m-1}} \phi_{l,k} \quad \forall p_m \in [p_e, p_{e+s}] \tag{A2}$$

$$r_{i,k} \leqslant \sum_{l} 0 \cdot x_{l,m} \cdot \phi_{l,k} + M(1-0) = M \quad \forall p_m \in [p_{e+s+1}, p_N] \tag{A3}$$

Hence, the three sets of constraints together will give:

$$r_{i,k} \leqslant \sum_{l=p_1}^{p_{e-1}} \phi_{l,k} \tag{A3}$$

For the constraint (28), one can similarly obtain:

$$\bar{r}_{i,k} \leqslant \sum_{l=p_{e+s+1}}^{p_N} \phi_{l,k} \tag{A4}$$

Also, constraint (29) gives:

$$r_{i,k} + \bar{r}_{i,k} + \sum_{l=p_e}^{p_{e+s}} \phi_{k,n} = 1 \tag{A5}$$

Hence, the constraints (A3)–(A5) together can ensure:

$$r_{i,k} = \sum_{l=p_1}^{p_{e-1}} \phi_{l,k} \tag{A6}$$

$$\bar{r}_{i,k} = \sum_{l=p_{e+s+1}}^{p_N} \phi_{l,k} \tag{A7}$$

References

Aboudolas, K., Papageorgiou, M., Kouvelas, A., Kosmatopoulos, E., 2010. A rolling-horizon quadratic-programming approach to the signal control problem in large-scale congested urban road networks. Transport. Res. Part C: Emerg. Technol. 18 (5), 680–694.

Chang, E.C., Cohen, S.L., Liu, C., Chaudhary, N.A., Messer, C., 1988. MAXBAND-86: program for optimizing left-turn phase sequence in multiarterial closed networks. Transport. Res. Rec. 1181, 61–67.

Chaudhary, N.A., Kovvali, V.G., Chu, C.-L., Kim, J., Alam, S.M., 2002. Software for Timing Signalized Arterials. Report FHWA/TX-03/4020-1, Texas Transportation Institute, the Texas A&M University System, College Station, Texas, September.

D'Ans, G.C., Gazis, D.C., 1976. Optimal control of oversaturated store- and forward transportation networks. Transport. Sci. 10, 1–19.

Gartner, N.H., Stamatiadis, C., 2004. Progression optimization featuring arterial-and route-based priority signal networks. J. Intell. Transport. Syst. 8 (2), 77–86.

Gartner, N.H., Stamatiadis, C., 2002. Arterial-based control of traffic flow in urban grid networks. Math. Comput. Model. 35 (5), 657–671.

Gartner, N.H., Assman, S.F., Lasaga, F., Hou, D.L., 1991. A multi-band approach to arterial traffic signal optimization. Transport. Res. Part B 25 (1), 55–74.

Hadi, M.A., Wallace, C.E., 1993. Hybrid genetic algorithm to optimize signal phasing and timing. Transport. Res. Rec. 1421, 104–112.

Kashani, H.R., Saridis, G.N., 1983. Intelligent control for urban traffic systems. Automatica 19, 191–197.

Li, J.Q., 2014. Bandwidth synchronization under progression time uncertainty. IEEE Trans. ITS 15 (2), 1–11.

Li, Z., 2012. Modeling arterial signal optimization with enhanced cell transmission formulations. J. Transport. Eng. 137 (7), 445–454.

Little, J.D.C., 1966. The synchronization of traffic signals by mixed-integer linear programming. Oper. Res. 14 (4), 568–594.

Little, J.D.C., Kelson, M.D., Gartner, N.H., 1981. MAXBAND: a program for setting signals on arteries and triangular networks. Transport. Res. Rec. 795, 40–46.

Liu, Y., Chang, G.L., 2011. An arterial signal optimization model for intersections experiencing queue spillback and lane blockage. Transport. Res. Part C: Emerg. Technol. 19 (1), 130–144.

Morgan, J.T., Little, J.D.C., 1964. Synchronizing traffic signals for maximal bandwidth. Oper. Res. 12 (6), 896–912.

Papageorgiou, M., 1995. An integrated control approach for traffic corridors. Transport. Res. Part C 3, 19–30.

Park, B., Messer, C.J., Urbanik, T., 1999. Traffic signal optimization program for oversaturated conditions: genetic algorithm approach. Transport. Res. Rec. 1683, 133–142.

Robertson, D.I., 1969. TRANSYT: A Traffic Network Study Tool. RRL Report LR 253, Road Research Laboratory, England.

Stamatiadis, C., Gartner, N.H., 1996. MULTIBAND-96: a program for variable-bandwidth progression optimization of multiarterial traffic networks. Transport. Res. Rec. 1554 (1), 9–17.

Stevanovic, A., Martin, P.T., Stevanovic, J., 2007. VisSim-based genetic algorithm optimization of signal timings. Transport. Res. Rec. 2035, 59–68.
Tian, Z., Urbanik, T., 2007. System partition technique to improve signal coordination and traffic progression. J. Transport. Eng. 133 (2), 119–128.
Wallace, C.E., Courage, K.G., Reaves, D.P., Shoene, G.W., Euler, G.W., Wilbur, A., 1988. TRANSYT-7F User's Manual: Technical Report. University of Florida, Gainesville, FL.
Yang, X., Chang, G.L., Rahwanji, S., 2014. Development of a signal optimization model for diverging diamond interchange. J. Transport. Eng., ASCE 2014, 140.
Yang, X., Lu, Y., Lin, Y., 2013. Interval optimization for signal timings with time-dependent uncertain arrivals. J. Comput. Civil Eng. http://dx.doi.org/10.1061/(ASCE)CP.1943-5487.0000356, 04014057.
Yin, Y., 2008. Robust optimal traffic signal timing. Transport. Res. Part B 42, 911–924.
Yun, I., Park, B., 2006. Application of stochastic optimization method for an urban corridor. In: Proceedings of the Winter Simulation Conference 3–6, pp. 1493–1499.